Observation of bubble dynamics within luminescent cavitation clouds: Sonoluminescence at the nano-scale

K. R. Weninger, C. G. Camara, and S. J. Putterman
Physics Department, University of California, Los Angeles, California 90095
(Received 14 July 2000; published 27 December 2000)

Measurements of acoustically driven cavitation luminescence indicate that this phenomenon is robust over a huge parameter space ranging from 10 kHz to >10 MHz. The minimum bubble radius achieved is an upper bound for the size of the light-emitting region and ranges from about 1 μm at 15 kHz to tens of nm at 11 MHz. Although lines can be discerned in the spectra of some cavitation clouds, they sit on top of a broadband continuum which can have greater spectral density in the ultraviolet than is observed for resonantly driven sonoluminescence from a single bubble.

DOI: 10.1103/PhysRevE.63.016310 PACS number(s): 78.60.Mq

A remarkable yet general aspect of continuous media is their ability to focus energy and stress when driven off equilibrium. Triboelectrification, fracture, and cavitation are some well-known examples. Cavitation, the formation and collapse of gas bubbles in liquids, spans a wide parameter space by itself [1]. The pressure drop in flow through a venturi tube creates bubbles which emit ultraviolet subnanosecond flashes of light as they collapse [2]. A single bubble can be trapped by a resonant sound field so as to emit a flash of light with each cycle of sound [3]. And the passage of a strong sound field through a fluid can create a cloud of light-emitting bubbles [4]. This transient-multibubble system is the arrangement in which sonoluminescence (SL) was first discovered in 1934 [5]. Our investigation of the range of the parameter space of transient SL indicates that it is possible to achieve visible light emission from regions with a radius of tens of nanometers. Light from resonantly driven bubbles displays spectra without spectral lines, whereas it is well known that light from transient SL can show such features, which have been interpreted to indicate a temperature of up to 5000 K [6]. We find, however, that the spectral lines sit on top of a broadband UV spectrum which appears to be hotter than resonantly driven SL. This observation along with measurements of bubble dynamics within cavitation clouds leads us to propose that conditions within transient bubbles are more extreme than those of resonantly driven SL from a single bubble, although their precise relationship to the spectral line thermometry experiments remains a mystery.

For this work we have generated light-emitting multibubble clouds by imposing acoustic fields driven at 27 kHz, 1 MHz, and 11 MHz into liquids. The bubble clouds form spontaneously in these systems when the acoustic amplitude is raised above a threshold. The light emission at all three frequencies is easily visible to the unaided eye with xenon dissolved in water and in some cases with other gases. Spectra for the emission of noble gas bubbles in water at the different frequencies are shown in Fig. 1 along with some single-bubble SL spectra for comparison. The broadband, featureless nature of the emission for these multibubble systems is remarkably similar to that of single-bubble SL and suggests a thermal emission. Two types of thermal emission that have been proposed as models of SL are (1) blackbody [7] and (2) bremsstrahlung from a plasma [8]. In view of the fact that the hotspot in the collapsed bubble is so small (indeed, smaller than the wavelength of light [7]), we shall assume that the hotspot is optically thin (i.e., transparent) and for the purpose of presentation will usually interpret spectra in terms of bremsstrahlung. In this case the spectral peak having an energy greater that 6 eV implies temperatures greater than 3 eV (36 000 K) for the interior of the bubble. The contrast between the continued increase in radiance below 350 nm for the multibubble systems containing xenon and the peak around 350–400 nm in the single-xenon-bubble radiance is the basis for the conclusion that the multibubble system is hotter.

In general, SL displays strong sensitivity to a number of experimental parameters [4]. Therefore, each apparatus allowed for control of the acoustic amplitude as well as the temperature, static pressure, and gas content of the liquid, although the method of sound generation was dramatically different. At 27 kHz the 5-mm-diam spherical titanium tip of the Contour Genesis System (Mentor Corp., California) is immersed in the liquid [9]. The tip is driven into longitudinal oscillations of up to 60 μm amplitude, establishing a dipole sound field in the liquid around the tip. Intense cavitation develops within a few mm of the tip where acoustic amplitudes are in the range of 3–10 bars. Note this cavitation is in the ''near field'' since at 27 kHz the wavelength of sound in water is about 5.5 cm. The gas of interest is continuously sparged into the liquid to maintain full saturation. The 1- and 11-MHz experiments were conducted in sealed volumes with the gas content of the liquid prepared in advance. The transducers were directed upward into the liquid toward a free surface. Bubbles form in the bulk of the liquid, which is now the ''far field'' of the acoustic transducer since the wavelengths of sound at 1 and 11 MHz are about 1.5 and 0.14 mm. The space above the free surface was filled with 1 bar of the gas of interest and connected to a gas-tight flexible bag to ensure 1 bar static pressure. At 1 MHz the transducer was the flat piezoceramic of the Silberg E.U.A. (Wells Johnson

 ©2000 The American Physical Society

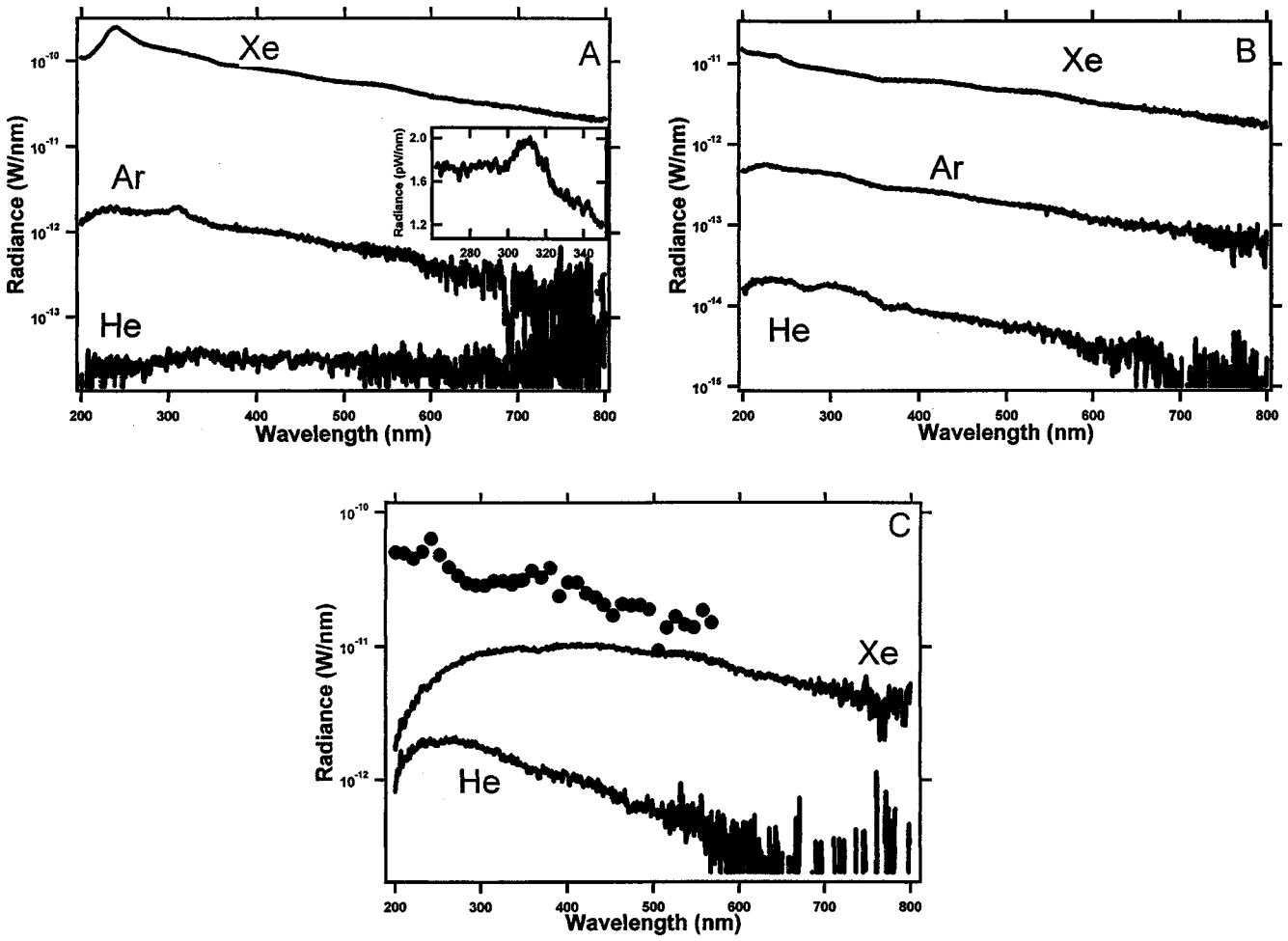

FIG. 1. Sonoluminescence spectra for noble gas bubbles in water: (A) Transient SL driven at 27 kHz with 30-μm displacement amplitude in 12C water. The inset shows a detail of the argon data. (B) Transient SL driven at 1 MHz and 7-bar pressure amplitude in 10C water. (C) Single-bubble SL driven at 33 kHz in 24C water at 3 torr gas saturation. The dots show transient SL driven at 11 MHz from 11C water saturated with xenon. All spectra were collected with light falling (through order-sorting filters) into a spectrometer (Acton 308i), which is read out by an intensified charge-coupled device (CCD) (Princeton Inst. IMAX) and fully calibrated against lamps of standard radiance. The resolution is 12 nm full width at half maximum (FWHM) for all except helium in A and B which is 72 nm FWHM and 11 MHz xenon in C which is 60 nm FWHM. All data are corrected with geometric factors for total emission into 4π except (B), which is total emission into 4π per cm^3 of cloud volume. The difference in absolute radiance for single bubble SL reported here as compared to Ref. [26] is due to differences in driving amplitude as well as possible errors in the overall multiplicative factor due to geometry (about 4π) in the previous calibration procedure. We see no relative differences among various colors in the spectrum, and all values for photons per flash are in agreement. In particular, air at 150 torr at room temperature near 30 kHz is 3×10^5 photons per flash.

Co., Tucson, AZ). This medical instrument, which is used in external ultrasound-assisted liposuction, generates a sound beam filling the volume at pressure amplitudes of 5–10 bars. This sound field creates a diffuse cloud of small bubbles filling the volume, as is visible in the photograph in Fig. 2. For 11 MHz a spherical focused transducer (Precision Acoustic Devices, Inc.) of the sort in scanning acoustic microscopes was used. A 0.075-mm-diam hydrophone (Precision Acoustic Ltd.) characterized the focal volume to extend 4 mm in length with a beam waist of about 250 μm diameter about $\frac{1}{2}$ in. above the transducer face (diameter $\frac{3}{4}$ in.). Driving with 5 V rms (below the cavitation threshold), 7 bars acoustic pressure was recorded. We observed that at 75 V (implying 100 bars) the focal volume was filled with a very dense cavitation cloud (opaque under backlighting) which emitted light easily visible to the eye. The drive used was in excess of the maximum allowable for the 0.008-in.-thick piezoceramic element, and the resulting catastrophic failure limited the experiment to only a few minutes, although a spectrum was recorded as shown in Fig. 1.

SL from a single bubble trapped at the velocity node of a standing-wave sound field is the form of cavitation luminescence that is most amenable to detailed measurements. Light-scattering data indicate that a flash of light is emitted at a minimum radius when the bubble contents have been compressed to their van der Waals hard core [10]. In order to compare resonantly driven SL to transient SL, we have measured bubble radii for the 27-kHz and 1-MHz systems. These bubble clouds were viewed with a long-distance microscope (Zeiss Achromat S 2.5×) and backlit with a 100-fs (up to 0.5

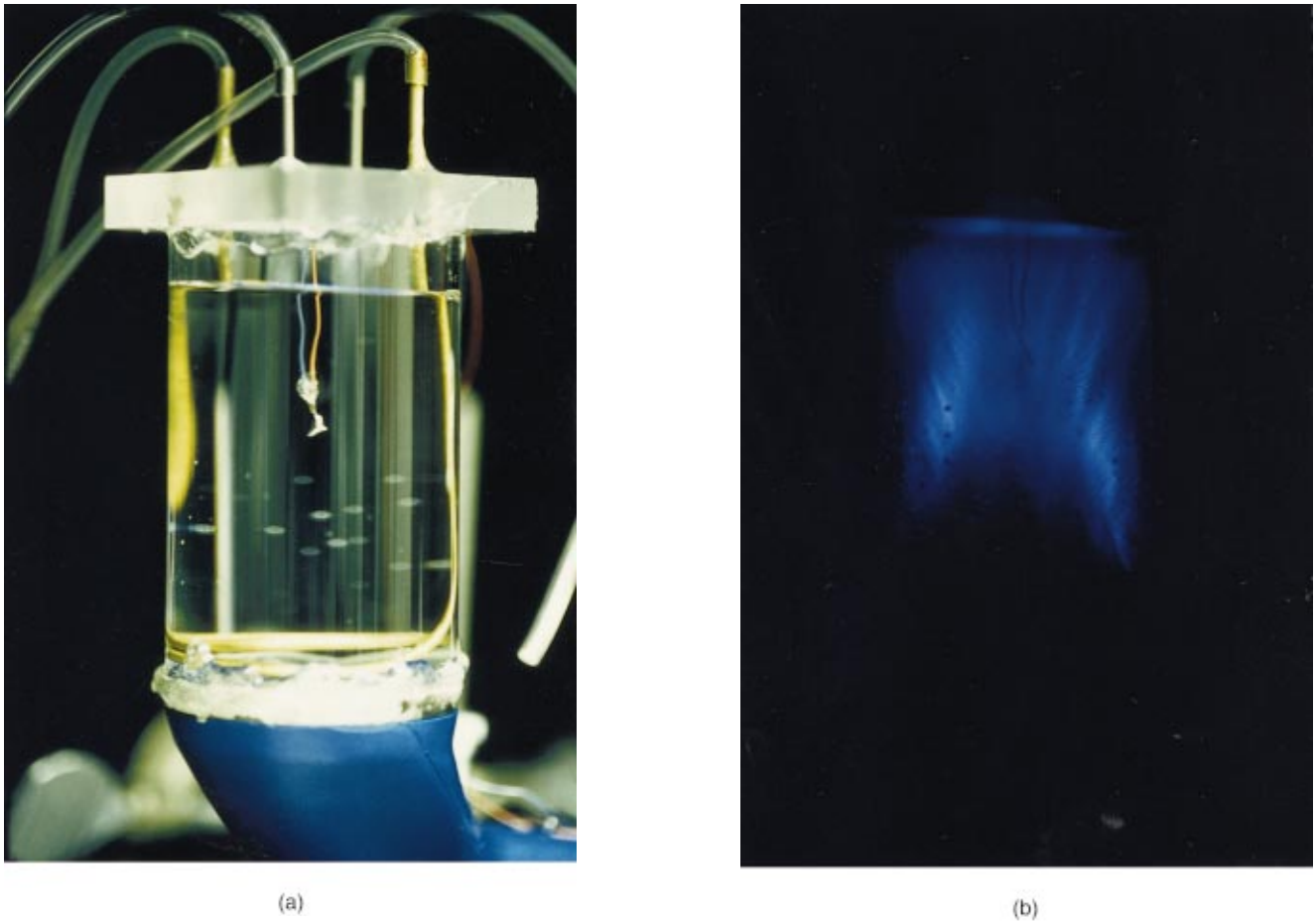

FIG. 2. (Color) Transient SL at 1 MHz. (a) shows a photograph of the apparatus. The transducer is in the blue handle and the quartz tubing is 50 mm in diameter. In (b) the light emitted by the xenon bubble cloud in water is imaged with a 1-min exposure (400 ASA slide film) with no external lighting.

mJ) 400-nm flash from a regeneratively amplified Ti:sapphire laser (see Fig. 3). The laser pulse was triggered (± 15 ns) from the sound field. Many samples at given phases of the sound field were acquired to build an ensemble of bubble sizes as a function of time within an acoustic cycle. At 1 MHz, all bubbles observed were spherical, but no definite phase behavior was seen probably due to the disturbance of the free surface by streaming fluid leaving the transducer. At 27 kHz, many spherical bubbles were observed which seemed to vary in size in phase with the sound field as shown in Fig. 4. In addition, larger nonspherical bubbles were seen, but we could not observe any dynamical trends phased with the sound field for them.

At sound phases near the moment of SL as determined by a photomultiplier tube, one also observes the presence of outgoing shock waves centered on the smaller bubbles at 27 kHz [see Fig. 3(c)][10,11]. We have used the observation of the shocks as a timing device for dynamical measurements of the natural ringing of these bubbles after the runaway implosion. This motion of the bubbles is a critical indicator of their ambient radius R_0, (the bubble radius for 1 bar pressure static and no driving sound). Under the assumption that the shock is emitted at the moment of maximum compression and in the approximation that the shock travels at the liquid sound speed, we have measured bubble radii at times after the collapse minimum radius as shown in Fig. 4(b). The sphericity of the shocks allowed positive identification of the bubble at the center of the shock as their source. Also shown are comparisons to solutions of the Rayleigh-Plesset (RP) equation [12].

The Rayleigh-Plesset equation of bubble dynamics provides an excellent description of the expansion and the beginning of the runaway collapse of a single acoustically driven bubble. The key input parameters are the ambient radius and the amplitude of the sound field at the bubble. The derivation of this equation assumes that the velocity of the bubble wall is small compared to the various speeds of sound [12]. As this condition is violated at and near the moment of light emission, the RP equation cannot be trusted to explain the properties of the flash or emitted shock waves.

In Fig. 4 the RP equation has been compared to the pulsations of bubbles within a cavitation cloud. We find that within these multibubble clouds there exists a set of spherical bubbles which are responding to the imposed sound field in the manner described by the RP model of bubble motion. It appears that for single bubbles and clouds of bubbles SL is emitted at the termination of a runaway implosion. In addition, we measure the sound fields to be 2–6 bars (27 kHz)

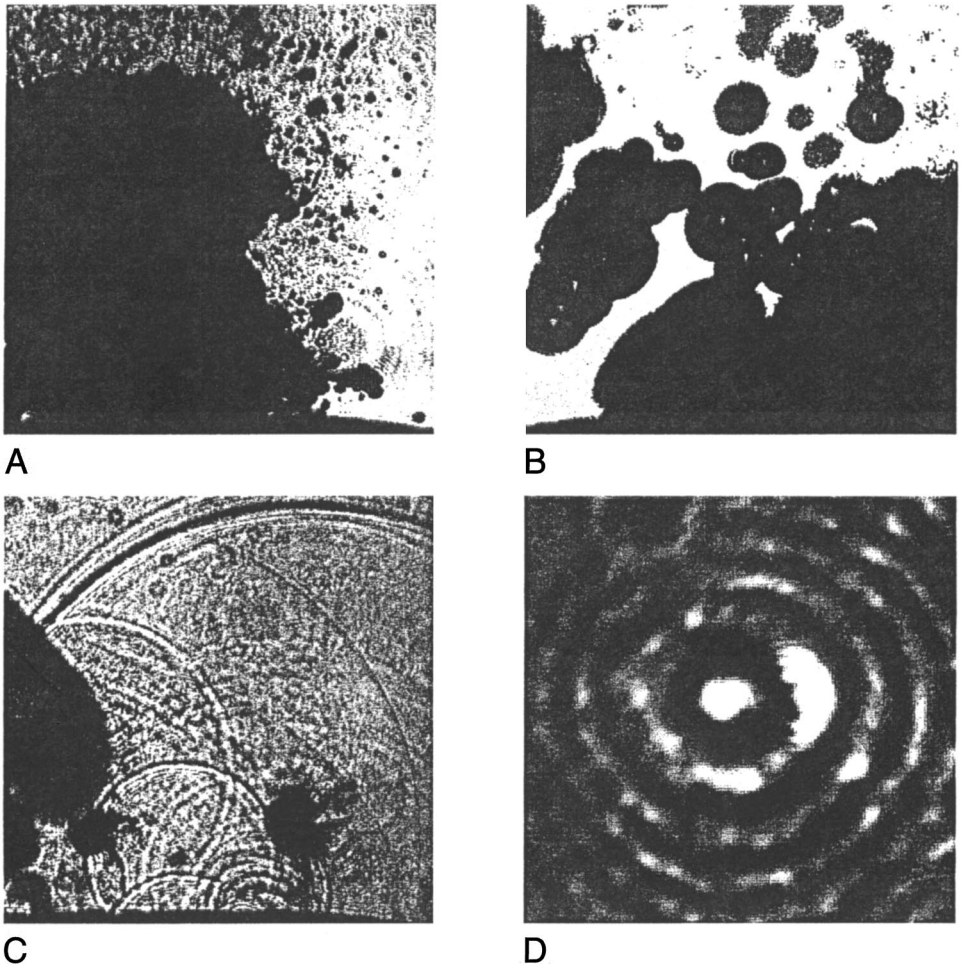

FIG. 3. Microscope images of bubbles within argon cavitation clouds in water driven at 27 kHz (A–C) and 1 MHz (D). Frames (A)–(C) are acquired at definite phases of the acoustic cycle indicated as 5, 27, and 36 μs, respectively [keyed to Fig. 4(A) time axis]. Along the lower edge of these images, the end of the transducer tip is visible. After tens of hours of use, these 27-kHz tips show significant ''cavitation damage.'' The full edge of these images represent 1.1 mm (A–C) and 70 μm (D).

and 6–8 bars (1 MHz) and observe dynamics indicating ambient radii of 3–6 μm (27 kHz) and 0.3–0.6 μm (1 MHz). These bubbles are driven harder than is achievable in single-bubble SL, which may account for the hotter spectrum observed. An upper bound on the size of the emitting region is given by the minimum collapse radius of these bubbles, which is determined from the van der Waals hard-core volume [for argon (xenon) this is the ambient radius divided by 8.8 (7.6)]. This hard-core volume yields radii of about 350–700 nm (27 kHz) and 35–70 nm (1 MHz). In light of the similar spectrum observed at 11 MHz, we extrapolate this line of reasoning based on RP dynamics to bubbles driven at 11 MHz with 100 bars driving pressure to estimate R_0 in the range 25–750 nm. RP solutions show that for smaller R_0, surface tension prevents these bubbles from expanding, yielding the lower limit. For $R_0 > 50$ nm the solutions show a dramatic subharmonic response [13], although some strong collapses do occur. The upper limit we propose follows from the observation in single-bubble SL that luminescence is accompanied by supersonic implosions and expansion ratios (radius from which implosion begins, R_0) of around 10. For these strong collapses, we find that RP predicts supersonic motion for R_0 less than 1–3 μm and expansion ratios of at least 10 for R_0 less than about 3/4 μm. This range of R_0 yields a collapsed light-emitting region characterized by 3–130 nm. (Note that if the more restrictive $R_0 = 50$ nm is assumed, the emission region range becomes 3–7 nm.)

Our observation of multibubble SL conditions hotter than single-bubble SL can be contrasted with the large body of work which finds temperatures of 2500–5000 K using comparative rate thermometry [14] and spectroscopic thermometry of line emissions [15,16] observed in some multibubble systems. We have duplicated many of the line emissions observed in previous experiments. In Fig. 1, a line at 310 nm commonly ascribed [17] to OH* emission is visible in the 27-kHz, argon in water data. We also measured the ratio of the line intensity to the continuum intensity of the 589-nm atomic sodium doublet from argon-saturated 0.2 M salt (NaCl) water to be 3.0 at 27 kHz and 0.2 at 1 MHz [18,19]. Figure 5 displays our observation of the (Swan) rotovibrational bands of C_2 seen in 27-kHz dodecane multibubble clouds [15]. In fact, the ratio of line amplitudes in the C_2 bands used to generate a temperature measurement of about 5000 K in Ref. [15] are verified by our data.

The means whereby selected lines are generated has not been clearly established. Sodium lines have been ascribed to the interaction of radicals (created by the collapsed bubble) with sodium in solution to generate excited states of sodium atoms [18]. They have also been ascribed to droplets of water sodium solution that find their way into the bubble to be excited by the SL implosion [19]. Use of the swan lines for temperature has been questioned since around 5000 K disso-

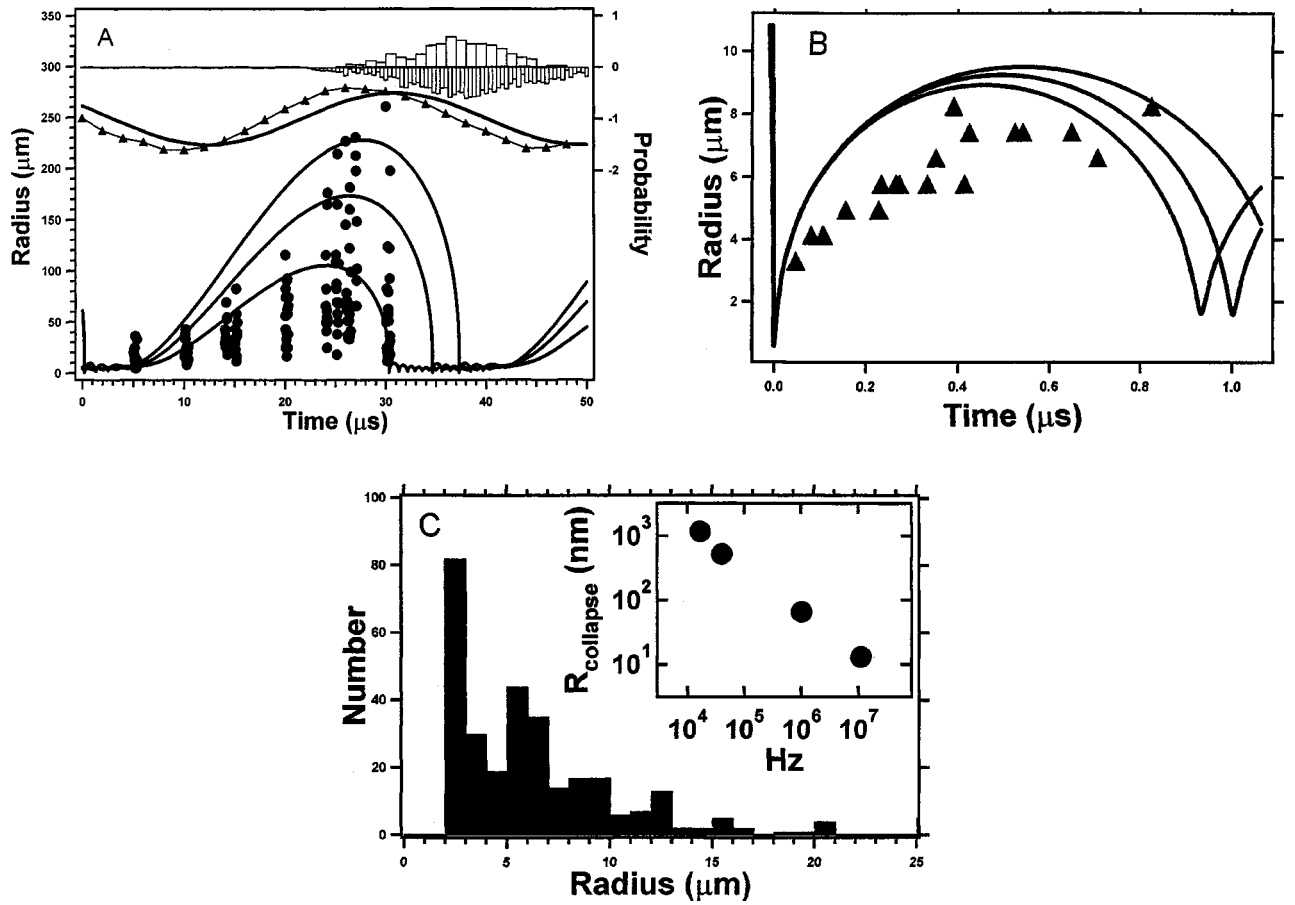

FIG. 4. Dynamics of bubbles within argon cavitation clouds in water at 12C. (A) Dots show radius measurements of all spherical bubbles observed in snapshots of the sort in Fig. 3 (some at higher magnification) phased to the driving sound at 27 kHz. The triangles show the microscopically imaged displacement of the transducer tip (on the micron axis). The solid lines show the bubble motion predicted by the RP model for $R_o = 5$ μm and $P_a = 2,3,4$ bars as well as the driving pressure (sine wave, arbitrary units) used to generate the radial theory values. The phase predicted between this pressure and tip displacement for the near field of the sound wave is used to align the theory curves on the time axis of the data. The positive going histogram bars (keyed to the right axis) show the observed probability of a microscope snapshot to contain at least one shock wave at various phases of the sound, whereas the negative histogram bars (arbitrary units) show the average output of a photomultiplier tube measuring the SL. Note the emission of light and shock waves coincides with the bubble implosions. (B) Bubble radius vs time derived using emitted shocks for timing. We assume the shock is emitted at time zero and travels at the liquid sound speed c. Then the radius of the shock divided by c determines a time to which the observed bubble radius is assigned. Also shown are the RP solutions from (A), but now the phase is adjusted so the moment of collapse is time zero. Because the acoustic pressure is determined independently, this bubble motion constrains the ambient radii to a range of about 3–6 μm. (C) Histogram of radii of all bubbles observed at 1 MHz. We interpret the peak near 6 μm to indicate a typical maximum radius for these bubbles. The peak at 2 μm shows that there are many resolution-limited observations also. For the measured acoustic pressure, RP theory predicts R_o of 0.3–0.6 μm yield maximum radii of 4–8 μm. The inset shows the trend of the collapsed minimum radius R_{collapse} ($=R_o/8.8$ for argon) vs driving frequency we observe for light-emitting bubbles using both single-bubble and cavitation cloud experiments.

ciation plays a role [20]. In response to this concern, SL temperatures of around 5000 K have also been obtained from chromium lines [16].

However the lines form, it must be emphasized that in some cases the 5000-K spectral lines are accompanied by a broadband spectrum extending up to photon energies of 6 eV. The difference in the temperature of the lines and the continuum depends upon how the continuum is modeled. Consider, for instance, the specific case of xenon in dodecane (Fig. 5). A blackbody fit yields a temperature of 7600 K, whereas a bremsstrahlung fit yields about 20 000 K. Perhaps the temperature of the lines and the continuum have a different origin [20,21]. The dependence of the spectral line determined temperatures on parameters such as the polytropic ratio or thermal conductivity of the gas or vapor pressure of the liquid suggests that they do reflect a measurement of the heating of a gas in a collapsing bubble [16]. It has been suggested that a distribution of bubble sizes may account for the different temperatures [20]. The energy available for focusing inside a collapsed bubble is determined by $(R_m/R_0)^3$ where R_m is the maximum radius. To achieve an average energy that is a factor of 6 smaller than 3 eV requires a larger R_0 (about 100–200 μm). Such bubbles should achieve their minimum radius about 5 μs earlier in the sound period than the 5-μm bubbles we observed. We have time resolved the spectral emission by using a gated ICCD for

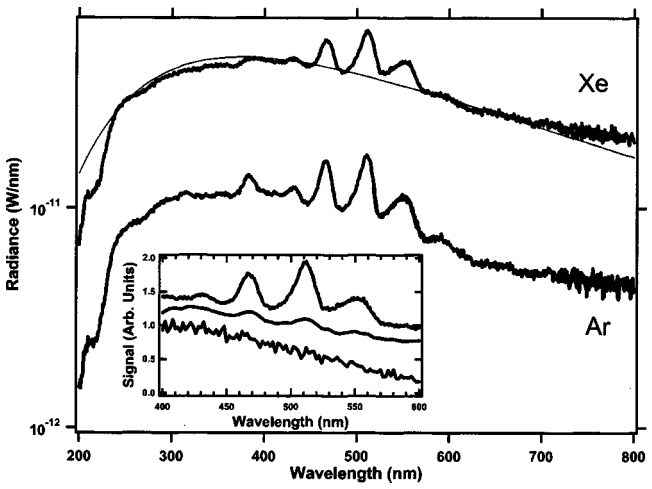

FIG. 5. SL spectra from argon and xenon cavitation clouds in 3C dodecane driven at 27 kHz with 30-μm displacement amplitude (12 nm FWHM). The falloff in the UV (below 260 nm) is due to absorption in the liquid which has not been corrected. The inset shows the C_2 Swan line transition for xenon dissolved in dodecane using (top to bottom): 27-kHz transient SL, 290-torr wall bubble SL (10 nm FWHM) [24] and SBSL at 150 torr (3 nm FWHM) [23]. The continuum of the 27-kHz xenon data has been fit by a 7600-K blackbody spectrum. Analysis of the line intensities by the model of [15] indicates a temperature of 4500 K for the same 27-kHz xenon data.

detection and find the line emission coincident with the continuum emission (1-μs resolution). All temperature measurements from spectral line emission are made in systems utilizing an oscillating solid probe immersed in the liquid to generate the bubble cloud. Perhaps the presence of the solid surface either rubbing the liquid or inducing jetting from bubbles which collapse near the surface [1,6,22] generates 5000-K conditions. In this spirit we point out that for a system of xenon in dodecane with acoustic frequencies near 30 kHz (see Fig. 5), single-bubble SL shows no C_2 emission [23], a single bubble near a solid surface shows slight C_2 emission [24], and multibubble SL (driven by an oscillating solid probe) shows stronger C_2 emission, although all three systems display a similar broadband, strongly ultraviolet continuum.

Except for the appearance of occasional spectral lines, clocklike SL from a single pulsating bubble and SL from a cavitating cloud of bubbles are remarkably similar. In each case the flash widths are subnanosecond [25,26], and the spectra are broadband, extending out to at least 6 eV. Interest in SL has been driven by the remarkably short durations of the emitted flashes, ranging down to 30 ps for a well-degassed solution of air in water resonantly driven at 34 kHz [26]. It will be interesting to determine if the length of the flashes from 11-MHz cavitation can be even shorter. Since transient SL is exempt from the requirements of steady-state motion (such as diffusional equilibrium [27]), it appears possible to reach even more extreme conditions. Three equilibrium models of the spectrum have been discussed: (1) blackbody [7], (2) bremsstrahlung [8], both in the weak and strong ionization limits, and (3) pressure-broadened atomic or molecular bound-state emissions of a nonionized, 5000-K gas [6,15,16,20,28]. The universal structure of the continuum suggests blackbody [7] if the hot spot is opaque and bremsstrahlung if it is sufficiently small so as to be transparent. It remains to be seen whether the more detailed formulation of process (3) can explain (a) the similarity of the spectra observed and (b) the means whereby a temperature of 1/2 eV yields a thermal spectrum with a peak beyond 6 eV. Regardless of which theory is correct, the stronger UV emission for multibubble SL than single-bubble SL implies more extreme conditions, which, furthermore, have been shown to facilitate the observation of SL down to dimensions of tens of nanometers.

We thank K. Suslick and B. Silberg for useful discussions, and also R. von Gutfeld for suggesting use of the P.A.D. device to search for SL at 11 MHz. The generous loan of equipment from Mentor Corp. and Wells Co. is appreciated. Research supported by DARPA, DOE (Engineering Research), and NSF (Division of Atomic, Molecular and Optical Physics).

[1] T. G. Leighton, *The Acoustic Bubble* (Academic, San Diego, CA, 1994); C. E. Brennen, *Cavitation and Bubble Dynamics* (Oxford University Press, New York, 1995); R. E. Apfel, Methods Exp. Phys. **19**, 355 (1981).

[2] F. B. Peterson and T. P. Anderson, Phys. Fluids **10**, 874 (1967); K. R. Weninger, C. G. Camara, and S. J. Putterman, Phys. Rev. Lett. **83**, 2081 (1999).

[3] P. R. Temple, MS thesis, University of Vermont, 1970; D. F. Gaitan *et al.*, J. Acoust. Soc. Am. **91**, 3166 (1992); B. P. Barber *et al.*, Phys. Rep. **281**, 65 (1997); S. J. Putterman and K. R. Weninger, Annu. Rev. Fluid Mech. **32**, 445 (2000).

[4] A. J. Walton and G. T. Reynolds, Adv. Phys. **33**, 595 (1984).

[5] H. Frenzel and H. Schultes, Z. Phys. Chem. Abt. B **27**, 421 (1934).

[6] K. S. Suslick *et al.*, Philos. Trans. R. Soc. London, Ser. A **357**, 335 (1999).

[7] B. E. Noltingk and E. A. Neppiras, Proc. Phys. Soc. London, Sect. B **63**, 674 (1950); P. Gunther, E. Heim, and H. U. Borgstedt, Z. Elektrochem. **63**, 43 (1959); D. Srinivasan and L. V. Holroyd, J. Appl. Phys. **32**, 446 (1961); G. Vazquez, C. Camara, S. J. Putterman, and K. Weninger (unpublished). Optical microscopy of the hot spot indicates a resolution-limited bound on its diameter as 1 μm for single-bubble SL at 40 kHz [S. Putterman, P. G. Evans, G. Vazquez, and K. Weninger (unpublished)]. If an understanding of how a photon mean free path can be sufficiently small within such a light-emitting region so that equilibrium between matter and radiation can be established, then blackbody models will deserve renewed consideration (see, for example, Y. B. Zel'dovich and Y. P. Raizer, *Physics of Shock Waves and High-Temperature Hydrodynamic Phenomena* (Academic, New York, 1966).

[8] T. K. Saksena and W. L. Nyborg, J. Chem. Phys. **53**, 1722 (1970); C. C. Wu and P. H. Roberts, Phys. Rev. Lett. **70**, 3424 (1993); W. C. Moss *et al.*, Science **276**, 1398 (1997); S. Hilgenfeldt, S. Grossmann, and D. Lohse, Nature (London) **398**, 402 (1999).

[9] K. R. Weninger, C. G. Camara, and S. J. Putterman, Clin. Plast. Surg. **26**, 463 (1999).

[10] K. R. Weninger, P. G. Evans, and S. J. Putterman, Phys. Rev. E **61**, R1020 (2000); K. Weninger, B. P. Barber, and S. J. Putterman, Phys. Rev. Lett. **78**, 1799 (1997).

[11] T. J. Matula *et al.*, J. Acoust. Soc. Am. **103**, 1377 (1998); J. Holzfuss *et al.*, Phys. Rev. Lett. **81**, 5434 (1998); Z. Q. Wang *et al.*, Phys. Rev. E **59**, 1777 (1999); R. Pecha and B. Gompf, Phys. Rev. Lett. **84**, 1328 (2000).

[12] A. Prosperetti, Rendiconti S.I.F. **93**, 145 (1984); R. Löfstedt *et al.*, Phys. Fluids A **5**, 2911 (1993).

[13] P. Smereka, B. Birnir, and S. Banerjee, Phys. Fluids **30**, 3342 (1987); A. Prosperetti, J. Acoust. Soc. Am. **57**, 810 (1975). Motivated by concerns regarding diagnostic imaging, ultrasound numerical studies of the RP theory for bubble motion of the sort found in these experiments are available in C. C. Church, *ibid.* **83**, 2210 (1988); H. G. Flynn and C. C. Church, *ibid.* **84**, 985 (1988).

[14] K. S. Suslick, D. A. Hammerton, and R. E. Cline, J. Am. Chem. Soc. **108**, 5641 (1986).

[15] E. B. Flint and K. S. Suslick, Science **253**, 1397 (1991); E. B. Flint and K. S. Suslick, J. Am. Chem. Soc. **111**, 6987 (1989); Y. T. Didenko, W. B. McNamara, and K. S. Suslick, J. Phys. Chem. A **103**, 10783 (1999).

[16] W. B. McNamara, Y. T. Didenko, and K. S. Suslick, Nature (London) **401**, 772 (1999); Y. T. Didenko, W. B. McNamara, and K. S. Suslick, Phys. Rev. Lett. **84**, 777 (2000).

[17] Y. T. Didenko and T. V. Gordeychuk, Phys. Rev. Lett. **84**, 5640 (2000); Y. T. Didenko and S. P. Pugach, J. Phys. Chem. **98**, 9742 (1994).

[18] E. B. Flint and K. S. Suslick, J. Phys. Chem. **95**, 1484 (1991).

[19] T. J. Matula *et al.*, Phys. Rev. Lett. **75**, 2606 (1995).

[20] L. S. Bernstein *et al.*, J. Phys. Chem. **100**, 6612 (1996).

[21] T. J. Matula and R. A. Roy, Ultrason. Sonochem. **4**, 61 (1997).

[22] L. A. Crum, J. Acoust. Soc. Am. **95**, 559 (1994).

[23] K. R. Weninger *et al.*, J. Phys. Chem. **99**, 14195 (1995).

[24] K. R. Weninger *et al.*, Phys. Rev. E **56**, 6745 (1997).

[25] T. J. Matula, R. A. Roy, and P. D. Mourad, J. Acoust. Soc. Am. **101**, 1994 (1997); B. Gompf *et al.*, Phys. Rev. Lett. **79**, 1405 (1998).

[26] R. A. Hiller, S. J. Putterman, and K. R. Weninger, Phys. Rev. Lett. **80**, 1090 (1998).

[27] M. M. Fyrillas and A. J. Szeri, J. Fluid Mech. **277**, 381 (1994); R. L. Lofstedt, K. Weninger, S. Putterman, and B. P. Barber, Phys. Rev. E **51**, 4400 (1995).

[28] K. Yasui, Phys. Rev. Lett. **83**, 4297 (1999).